J Mater Sci (2011) 46:681–687
DOI 10.1007/s10853-010-4791-y

# Magnetic and electrical properties of ordered 112-type perovskite $LnBaCoMnO_{5+\delta}$ (Ln = Nd, Eu)

**Asish K. Kundu · V. Pralong · B. Raveau · V. Caignaert**

Received: 6 July 2010 / Accepted: 23 July 2010 / Published online: 4 August 2010


**Abstract** Investigation of the oxygen-deficient 112-type ordered oxides of the type $LnBaCoMnO_{5+\delta}$ (Ln = Nd, Eu) evidences certain unusual magnetic behavior at low temperatures, compared to the $LnBaCo_2O_{5+\delta}$ cobaltites. The ordered $NdBaCoMnO_{5.9}$ depicts a clear paramagnetic to antiferromagnetic type transition around 220 K, whereas for $EuBaCoMnO_{5.7}$ one observes an unusual magnetic behavior below 177 K which consists of ferromagnetic regions embedded in an antiferromagnetic matrix. The existence of two sorts of crystallographic sites for Co/Mn and their mixed valence states favor the ferromagnetic interaction, whereas antiferromagnetism originates from the $Co^{3+}$–O–$Co^{3+}$ and $Mn^{4+}$–O–$Mn^{4+}$ interactions. Unlike the parent compounds, the present Mn-substituted phases do not exhibit prominent magnetoresistance effects in the temperature range 75–400 K.

## Introduction

Ordered 112-type perovskite cobaltites are increasingly recognized as materials of importance due to rich physics and chemistry in their layered structure [1–16]. Apart from colossal magnetoresistance effect, like manganites, the different form of cobaltites exhibit interesting phenomena including magnetic ordering, electronic phase separation, insulator–metal transition, large thermoelectric power at low temperature [1–10]. A few of these behaviors are of great interest because of their potential applications as read heads in magnetic data storage, oxidation catalyst, gas sensors, etc., and also in other applications depending upon their particular properties [1, 12–16]. The well-known oxygen-deficient cobalt perovskite $LnBaCo_2O_{5+\delta}$ (Ln = rare earth) is basically derived from the 112-type ordered $YBaFeCuO_{5+\delta}$ structure [17]. In the case of cobaltites for $\delta = 0$ the structure only consists of double pyramidal cobalt layers, whereas for $\delta > 0$ there will be $CoO_6$ octahedra as well as $CoO_5$ pyramidal layers containing the barium cations, interleaved with rare earth layers [1–11]. The discovery of large magnetoresistance (MR) in this type of structure has renewed great interest in 112-ordered cobaltites since 1997 [1].

Likewise, the existence of ordered oxygen-deficient perovskites $LnBaCo_{2-x}M_xO_{5+\delta}$ (Ln = rare earth and M = metal cations) with interesting magnetic properties has stimulated the research of doped 112-ordered cobaltites [18–23]. In fact, the magnetic and electron transport properties of this type of oxides are very sensitive to their oxygen stoichiometry and to their complex crystal chemistry [24–31]. Numerous studies performed on the doped 112-ordered cobaltites have shown that their fascinating physical behavior is complex, in connection with their large possibility for cation ordered–disordered phenomena and oxygen deficiency [18–31]. According to our knowledge for such systems, with mixed Co and Mn-cations at the B-site of the perovskite, only two compounds are reported till date, i.e., $YBaMnCoO_5$ [32] and $NdBaMnCoO_{5+\delta}$ [33]. The latter one (with $\delta = 0$, 1) has been investigated recently by Snedden et al. [33], who reported a tetragonal structure with *P4/mmm* space group (unit cell $a_p \times a_p \times 2a_p$) at room temperature. Moreover, the neutron diffraction studies show a G-type antiferromagnetic

A. K. Kundu
Indian Institute of Information Technology Design & Manufacturing, Dumna Airport Road, Jabalpur 482005, India

A. K. Kundu (✉) · V. Pralong · B. Raveau · V. Caignaert
Laboratoire CRISMAT, ENSICAEN UMR6508, 6 Boulevard Maréchal Juin, 14050 Caen Cedex 4, France
e-mail: asish.kundu@iiitdmj.ac.in

(AFM) structure for $\delta = 0$, but there is no evidence for magnetic ordering at low temperature for $\delta = 1$; although, a weak ferromagnetic (FM) ordering around 228 K was predicted for the latter one. In fact, no detailed investigation has allowed the FM ordering to be confirmed, so that it may be due to the presence of impurity phases [33]. There is certainly lack of supportive information on the FM phase below 228 K. Bearing these results in mind, we have investigated the effect of Mn-doping at the cobalt site in 112-ordered cobaltites. In contrast, the magnetic data reported for $NdBaCoMnO_6$ [33], we have defined the transition as AFM type and explored the low temperature region by means of isothermal magnetization to confirm the magnetic interaction. Herein, we also report a new 112-ordered phase $EuBaCoMnO_{5.7}$ that shows a magnetic transition at 177 K, with phase separation between an AFM matrix and FM domains below this temperature.

## Experimental procedure

The ordered $LnBaCoMnO_{5+\delta}$ (Ln = Nd, Eu) perovskites were synthesized by means of a soft-chemistry method. Stoichiometric amounts of metal oxides and nitrates $Ln_2O_3$, $Ba(NO_3)_2$–$H_2O$, $Co(NO_3)_2$–$6H_2O$, and $Mn(NO_3)_2$–$4H_2O$ were dissolved into distilled water and citric acid was added to the solution in the molar ratio. After adding citric acid into the solution, the mixture solutions were heated at 100 °C for few hours and evaporated at 150 °C to form an amorphous dry gel, which was decomposed at 800 °C for overnight to burn away the carbon and nitrogen residues. The powder samples were ground thoroughly and pressed into rectangular bars, and finally sintered at 1200–1320 °C in Ar flow (5 N) for 36 h in plate-type platinum crucible. Heating and cooling rates were kept slow (2 °C/min) to enable better *A*-cation and oxygen vacancy ordering. The parent compounds $LnBaCo_2O_{5+\delta}$ (Ln = Nd, Eu) were prepared by the conventional solid state reaction method as reported in the literature [1–8].

Small parts of the sintered bar were taken and ground to form fine powder to record the X-ray diffraction (XRD) pattern, using a Philips diffractometer employing Cu Kα radiation. The phases were identified by performing Rietveld [34] analysis in the $2\theta$ range of 5°–120° and the lattice parameters were calculated accordingly. Composition analysis was carried out by energy dispersive spectroscopy (EDS) analysis using a JEOL 200CX scanning electron microscope, equipped with a KEVEX analyzer. The oxygen stoichiometry was determined by iodometric titrations. The error in oxygen content was ±0.05.

Other pieces of the rectangular bars were taken for magnetization, resistivity, and thermopower measurements. A Quantum Design physical properties measurements system (PPMS) magnetometer was used to investigate the magnetic properties of the samples. The temperature dependence of the zero-field-cooled (ZFC) and field-cooled (FC) magnetization was measured in different applied magnetic fields. Hysteresis loops $M(H)$ were recorded at different temperatures. In the measurements of the ZFC magnetization, the sample was cooled from 300 to 10 K in zero-field, the field was applied at 10 K and the magnetization recorded on re-heating the sample. In the FC measurements, the sample was cooled (from 300 K) in the applied field to 10 K and the magnetization recorded on re-heating the sample, keeping the field applied. The electrical measurements were carried out on a rectangular-shaped ($6.90 \times 2.65 \times 2.20$ mm$^3$) sample by a standard four-probe method in the temperature range of 10–400 K. The electrodes on the sample were prepared by ultrasonic deposition method using indium metal.

## Results and discussion

### Structural analysis at room temperature

All the perovskite-based 112-ordered samples $LnBaCo_{2-x}Mn_xO_{5+\delta}$ (with Ln = Nd/Eu and $x = 0$, 1), confirm the single-phase, without any traces of impurities as shown in Fig. 1. The crystal structure adopted by ordered cobaltite $LnBaCo_2O_{5+\delta}$ (Ln = rare earth) has been reported to be either tetragonal *P4/mmm* ($a_p \times a_p \times 2a_p$), orthorhombic *Pmmm* ($a_p \times 2a_p \times 2a_p$ or $a_p \times a_p \times 2a_p$), or orthorhombic *Pmmb* ($a_p \times 2a_p \times 2a_p$). Here, $a_p$ refers to the basic cubic perovskite cell parameters (ca. 3.9 Å).

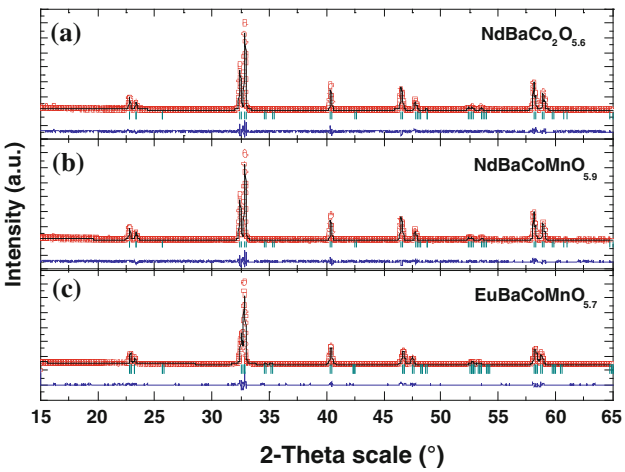


**Fig. 1** Rietveld analysis of XRD pattern for **a** $NdBaCo_2O_{5.6}$ **b** $NdBaCoMnO_{5.9}$, and **c** $EuBaCoMnO_{5.7}$ at room temperature. *Open symbols* are experimental data and the *dotted*, *solid*, and *vertical lines* represent the calculated pattern, difference curve and matched profile, respectively

**Table 1** Crystallographic data for (a) $NdBaCo_2O_{5.6}$ (b) $NdBaCoMnO_{5.9}$, and (c) $EuBaCoMnO_{5.7}$

| Compound | $NdBaCo_2O_{5.6}$ | $NdBaCoMnO_{5.9}$ | $EuBaCoMnO_{5.7}$ |
|---|---|---|---|
| Crystal system | Orthorhombic | Tetragonal | Orthorhombic |
| Space group | *Pmmm* (47) | *P4/mmm* (123) | *Pmmm* (47) |
| Cell parameters | $a = 3.900(1)$ Å | $a = 3.893(2)$ Å | $a = 3.884(2)$ Å |
| | $b = 7.826(2)$ Å | $c = 7.697(1)$ Å | $b = 3.893(2)$ Å |
| | $c = 7.611(1)$ Å | | $c = 7.653(1)$ Å |
| Cell volume | 232.32(2) Å$^3$ | 116.54(2) Å$^3$ | 115.70(3) Å$^3$ |
| $Z$ | 2 | 1 | 2 |
| $\chi^2$ | 2.07 | 3.22 | 7.10 |
| $R_B$ (%) | 9.71 | 6.42 | 8.93 |

The doubling in $c$ parameter is due to the ordering of Ln and Ba into layers. The cells doubling in $b$, and the transition from tetragonal to orthorhombic, have been suggested to arise from different orderings between oxygen and vacancies in the [$LnO_\delta$] layer [1–11]. The crystal structure for the phases $NdBaCo_2O_{5.6}$, $NdBaCoMnO_{5.9}$, $EuBaCo_2O_{5.5}$, and $EuBaCoMnO_{5.7}$, along with the oxygen content are in good agreement to the literature data [1–8]. The obtained cell parameters are presented in Table 1, which are deduced from XRD studies by Rietveld method.

## Magnetic properties of the parent compounds $LnBaCo_2O_{5.5+\delta}$ revisited

Figure 2 shows the ZFC and FC magnetization, $M(T)$, for $NdBaCo_2O_{5.6}$ and $EuBaCo_2O_{5.5}$ in an applied field of 1000 Oe which confirms the successive transitions from a PM state to a FM state and then to AFM state (mainly for Eu-phase), as previously reported in the literature [1, 2, 4–6, 8]. The existence of ferromagnetism for $EuBa\{Co^{III}\}_2O_{5.5}$ is in perfect agreement with the possibility of FM interactions due to intermediate spin state $Co^{3+}$ species (with the existence of two kinds of crystallographic sites) and for $NdBa\{Co^{III}\}_{1.8}\{Co^{IV}\}_{0.2}O_{5.6}$ also between $Co^{3+}$ and $Co^{4+}$ species, since the average oxidation state of cobalt is close to 3.10. Moreover, for $NdBaCo_2O_{5.6}$ in the low temperature regime several magnetic transitions noticed particularly in ZFC data a FM to AFM-type transition appeared around 210 K, but in FC data that transition is not so prominent although a small kink is observed. In the case of $EuBaCo_2O_{5.5}$, the AFM transition ($T_N \sim 245$ K) is clearly observed in both ZFC–FC data, yet the divergence between them persists down to low temperature. Hence, for both the systems, the magnetization value is non-zero below the AFM transition and there is a large irreversibility between the ZFC–FC magnetization data even at higher fields. This signifies some kind of short-range FM ordering in the low temperature AFM region. The isothermal, $M(H)$,

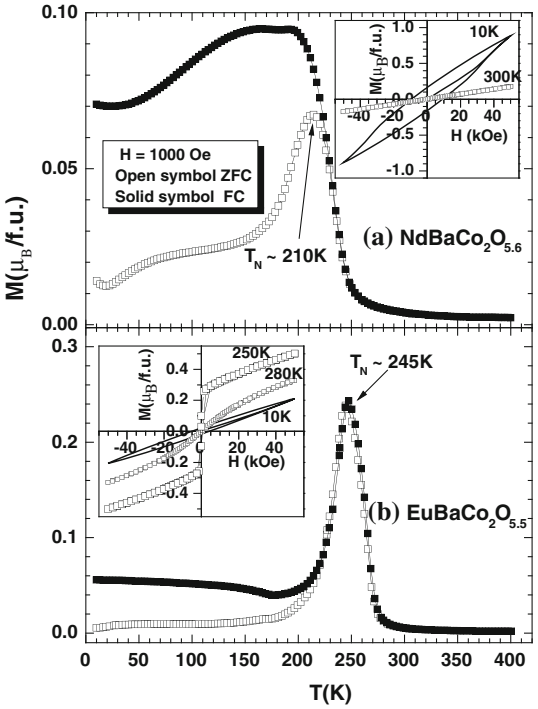


**Fig. 2** Temperature-dependent ZFC (*open symbol*) and FC (*solid symbol*) magnetization, $M$, of **a** $NdBaCo_2O_{5.6}$ and **b** $EuBaCo_2O_{5.5}$ ($H = 1000$ Oe). The *insets* show typical hysteresis curves at different temperatures

curves studied at different temperatures (insets of Fig. 2) also confirm this short-range FM ordering. One indeed observes a clear hysteresis loop for both compounds at 10 K and the hysteresis is rather smaller for $EuBaCo_2O_{5.5}$ when compared to $NdBaCo_2O_{5.6}$, with remanent magnetization ($M_r$) values of 0.024 and 0.16 $\mu_B$/f.u. and coercive fields ($H_C$) of ~4.1 and 9.5 kOe, respectively. The highest value of magnetic moment is only ~0.21 $\mu_B$/f.u. (0.87 $\mu_B$/f.u.) for Eu(Nd)-compound, which is less than the spin-only value of $Co^{3+}$-ions in the intermediate spin (IS) state. Below the magnetic ordering temperature (for both the phases) the obtained hysteresis loop signifies a typical FM state and at higher temperatures ($T > 200$ K) the $M(H)$ behavior is linear, corresponding to a PM state. Another interesting feature at low temperature is the unsaturated behavior of the $M(H)$ curve even at higher fields, which is in agreement with electronic phase separation as pointed out by several authors [5, 7, 8] and will not be discussed here.

## Magnetic properties of the Mn-doped phases: $LnBaCoMnO_{5+\delta}$

The $LnBaCoMnO_{5+\delta}$ (Ln = Nd, Eu) phases show a significant different transition temperature compared to their parent oxides $LnBaCo_2O_{5+\delta}$ [1, 2, 4–6, 8] and $LnBaMn_2O_{5+\delta}$ [35].

*Magnetic behavior of $NdBaCoMnO_{5.9}$*

Figure 3 exhibits the temperature-dependent ZFC and FC magnetization curves recorded at 1000 Oe for $NdBaCoMnO_{5.9}$. These are almost similar to that of $NdBaCoMnO_6$ reported by Snedden et al. [33]. In contrast to the report of the authors, in the temperature range of 10–400 K the system exhibits a clear PM to AFM transition around $T_N \sim 220$ K (shown by arrow mark in the figure). However, the magnetization value does not become zero below $T_N$, as expected for an AFM system and the value remains almost constant in the low temperature AFM state for both ZFC–FC data. Moreover, there is no such magnetic irreversibility between ZFC and FC data below $T_N$ unlike the parent phase $NdBaCo_2O_{5.6}$. However, the magnetization value increases rapidly at low temperature ($T < 80$ K), which may be due to the PM contribution from the Nd-cation as reported in the literature for some of the lanthanides [1, 4–6, 35]. Inset of Fig. 3 exhibits the inverse magnetic susceptibility versus temperature plot throughout the measured range. The latter follows a simple Curie–Weiss law in the $220 \leq T \leq 400$ K range and yields a PM Weiss temperature ($\theta_p$) of 11 K and an effective magnetic moment ($\mu_{eff}$) of $\sim$7.59 $\mu_B$/f.u. We have further studied the isothermal magnetization behavior, $M(H)$, of the ZFC sample recorded below the AFM transition to establish this behavior. Figure 4 shows the $M(H)$ curves at 10 and 100 K, exhibiting a typical feature of an AFM state below $T_N$ and above this temperature the $M(H)$ behavior is also linear corresponding to a PM state. Considering the potential of the couples $Co^{4+}/Co^{3+}$ and $Co^{3+}/Co^{2+}$ with respect to the couple $Mn^{4+}/Mn^{3+}$, it clearly appears that $Co^{3+}$ is reduced into $Co^{2+}$ in the presence of $Mn^{3+}$ according to the equation

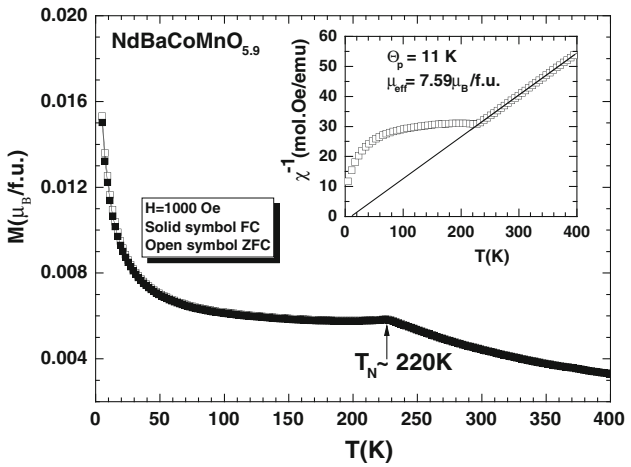


**Fig. 3** Temperature-dependent ZFC (*open symbol*) and FC (*solid symbol*) magnetization, $M$, of $NdBaCoMnO_{5.9}$ in an applied fields of 1000 Oe. *Inset* figure shows the inverse susceptibility, $\chi^{-1}$, versus temperature plot

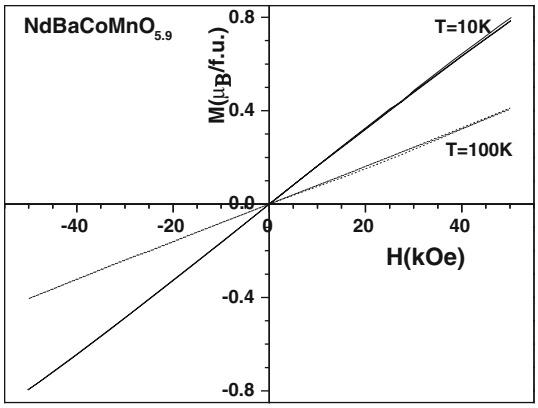


**Fig. 4** Magnetic field dependence of isothermal magnetization, $M(H)$, at two different temperatures for $NdBaCoMnO_{5.9}$

$Co^{3+} + Mn^{3+} \rightarrow Co^{2+} + Mn^{4+}$ [36–38]. As a result, the charge balance in this oxide can be formulated as $NdBa\{Co^{III}\}_{0.8}\{Co^{II}\}_{0.2}Mn^{IV}O_{5.9}$. Thus, the majority of interactions $Mn^{4+}$–O–$Mn^{4+}$, $Co^{3+}$–O–$Co^{3+}$, and $Co^{3+}$–O–$Mn^{4+}$ are predicted to be antiferromagnetic at low temperature, according to Goodenough–Kanamori rules [36, 37]. $Co^{2+}$–O–$Mn^{4+}$ interaction might be ferromagnetic, but this requires an ordering of the $Co^{2+}$ and $Mn^{4+}$ species, as reported for the double perovskite $La_2MnCoO_6$ [39], which is not the case for the present compound. The $Co^{2+}$–O–$Co^{3+}$ interactions may be either ferro- or anti-ferromagnetic, but in any case, they should bring a very low contribution, due to the low $Co^{2+}$ content. This behavior is different from parent $NdBaCo_2O_{5.6}$ compound, which exhibits FM interaction between $Co^{3+}$ and $Co^{4+}$ ions according to Goodenough–Kanamori rules [36].

*Magnetic behavior of $EuBaCoMnO_{5.7}$*

Bearing in mind the complex magnetic properties observed for $EuBaCo_2O_{5.5}$ and the strong AFM interactions in $NdBaCoMnO_{5.9}$, the possibility of a similar magnetic interaction with mixed Co-Mn system $EuBaCoMnO_{5.7}$ has been investigated in details. For as-prepared (in argon atmosphere) sample a large oxygen deficiency is observed, leading to the chemical formula $EuBa\{Co^{III}\}_{0.4}\{Co^{II}\}_{0.6}Mn^{IV}O_{5.7}$. The temperature-dependent ZFC–FC magnetization, $M(T)$, is measured in the range of 10–400 K under the applied fields of 100, 1000, and 5000 Oe (Fig. 5). With decreasing temperature the FC magnetization curve depicts a steep increase of the magnetization around 177 K followed by a small kink at 130 K. The FC data suggest a PM to FM-like transition $T_C \sim 177$ K, yet the highest obtained moment is only 0.06 $\mu_B$/f.u. (at $H = 5000$ Oe) and there is no saturation in the magnetization data down to low temperature. Moreover, the ZFC–FC curves exhibit a significant thermo-magnetic irreversibility below $T_C$ even at

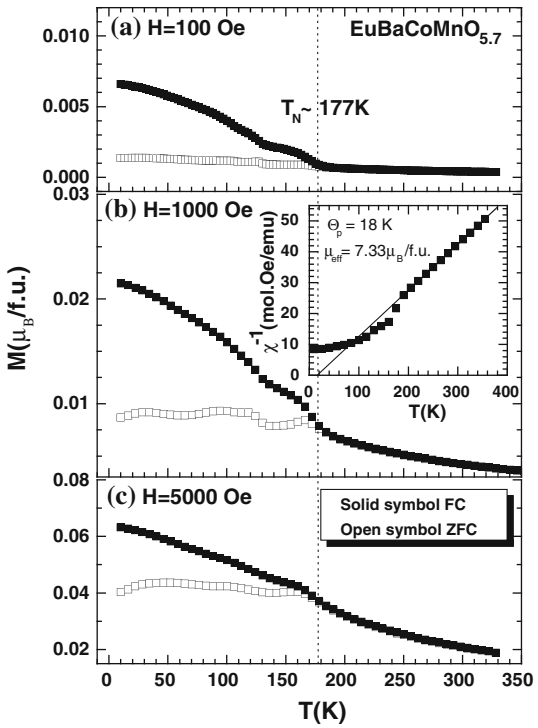


**Fig. 5** Temperature-dependent ZFC (*open symbol*) and FC (*solid symbol*) magnetization, $M$, of $EuBaCoMnO_{5.7}$ at different applied fields. **a** $H = 100$, **b** $H = 1000$ (*inset* shows inverse susceptibility, $\chi^{-1}$, versus temperature plot), and **c** $H = 5000$ Oe

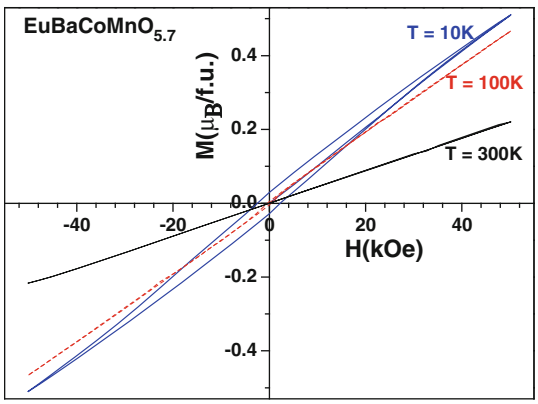


**Fig. 6** Magnetic field dependence of isothermal magnetization at three different temperatures for $EuBaCoMnO_{5.7}$

higher fields. It must also be emphasized that though the system becomes FM-like below 177 K, the magnitude of the magnetic moment as well as the ZFC–FC behavior (at higher fields) do not justify the long-range FM ordering or a true FM behavior. Indeed, the parent manganite $EuBaMn_2O_5$ phase also exhibits a magnetic transition around 150 K, yet for $EuBaMn_2O_6$ the transition is around 260 K. The magnetic state for $EuBaMn_2O_6$ is explained by inhomogenous ferromagnetism, whereas for $EuBaMn_2O_5$ as FM-type [35]. In order to clarify the FM-like state in $EuBaCoMnO_{5.7}$ the isothermal magnetization behavior, $M(H)$, at three different temperatures has been investigated as shown in Fig. 6. The $M(H)$ curve at 10 K depicts a prominent hysteresis loop with a remanent magnetization, $M_r$, and coercive field, $H_C$, values of 0.03 $\mu_B$/f.u. and 2.4 kOe, respectively, indicating a FM-like state. The hysteresis loop persists up to 100 K (see Fig. 6), though the $H_C$ ($\sim$0.4 kOe at 100 K) decreases with increasing temperature and above $T_C$ the $M(H)$ behavior is linear akin to PM state ($T = 300$ K). Nevertheless, the maximum value of the magnetic moment measured in 50 kOe is only 0.5 $\mu_B$/f.u. at 10 K, which is much smaller than the value expected for Co and Mn ions. The weak FM-like feature of $EuBaCoMnO_{5.7}$ at low temperature resemble with the magnetization obtained due to canting of the magnetic spin alignment in the G-type AFM structure as pointed out by several authors for 112-ordered cobaltites [3, 4, 10]. It is worth pointing out that at low temperature the magnetization value does not saturate even at higher fields. This is due to a superposition of a quite large AFM state and a small region of FM state similar to the phases $EuBaCo_{1.92}M_{0.08}O_{5.5-\delta}$ with M = Zn, Cu [21]. Hence, the obtained smaller value of magnetic moment for $EuBaCoMnO_{5.7}$ below $T_C$ can be explained by the appearance of electronic phase separation, i.e., the presence of small FM domains inside the AFM matrix. Indeed, in this phase the $Co^{2+}$ content has increased with respect to the $NdBaCoMnO_{5.9}$ phase, and the number of $Co^{2+}$–O–$Co^{3+}$ interactions is significantly larger. Thus, if the latter are FM at low temperature, as observed for $EuBaCo_2O_{5.33}$ [8] this could explain that there is a strong competition between positive $Co^{2+}$–O–$Co^{3+}$ FM interactions and negative $Mn^{4+}$–O–$Mn^{4+}$ and $Co^{2+}$–O–$Co^{2+}$ AFM interactions, whereas the FM interactions would dominate over AFM at higher fields. But, the contribution of AFM interaction is not negligible; hence, the isothermal $M(H)$ exhibits an unsaturated hysteresis behavior supporting the electronic phase separation model [21, 40, 41].

## Electron transport properties

The temperature dependence of the electrical resistivity ($\rho$) behavior for $LnBaCo_{2-x}Mn_xO_{5+\delta}$ (Ln = Nd, Eu and $x = 0$, 1) samples is shown in Fig. 7. The parent cobaltites show the well-known insulator–metal transition in the proximity of 350 K as reported in the literature [1, 2, 4, 6, 8]. In contrast for the Mn-substituted phases the insulator–metal transition completely disappears throughout the temperature range 60–400 K quite similar to $YBaMnCoO_5$ phase [32]. With decreasing temperature the resistivity increases for $NdBaCoMnO_{5.9}$ and $EuBaCoMnO_{5.7}$ samples

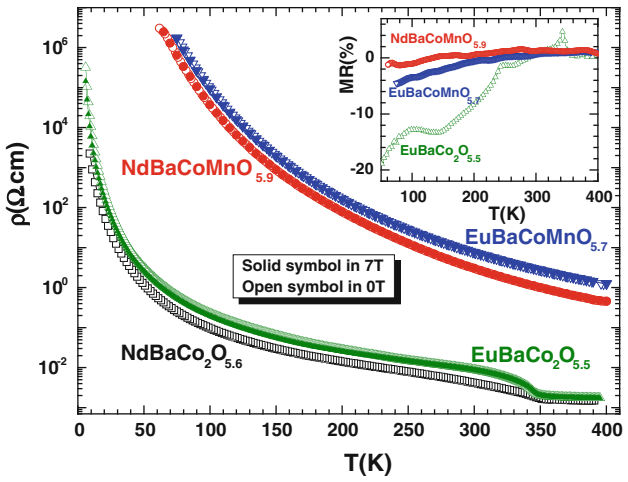


**Fig. 7** Temperature-dependent electrical resistivity, $\rho$, of $LnBaCo_{2-x}(Mn)_xO_{5+\delta}$ with Ln = Nd and Eu in the presence (*solid symbol*) and absence (*open symbol*) of magnetic field 7 Tesla. The *inset* figure shows magnetoresistance, MR(%), with the variation in temperature

and the value is very high at low temperature, crossing the instrument limitations below 60 K. The rapid increase in temperature coefficient of resistivity ($d\rho/dT$) from room temperature to low temperature signifies the insulating behavior. Thus, none of Mn-doped samples show an insulator–metal transition like the parent phases. The highest value of the resistivity at room temperature is observed for $EuBaCoMnO_{5.7}$. This is due to the smaller A-site cation radius for $EuBaCoMnO_{5.7}$ when compared to $NdBaCoMnO_{5.9}$. With decreasing the rare earth ion size the band gap between the valence and the conduction band increases, as a result resistivity increases. At this point, it is important to mention that since the $EuBaCoMnO_{5.7}$ shows a prominent magnetic ordering below 177 K, so we have also investigated the magnetoresistance effect in an applied field of 70 kOe. In a magnetic field, $\rho(T)$ does not show a large change in the resistivity behavior, in contrast to parent cobaltites, except a slight decrease in the magnitude is noticed at low temperature. Therefore, we have calculated the magnetoresistance (MR) as, $MR(\%) = [\{\rho(7) - \rho(0)\}/\rho(0)] \times 100$, where $\rho(0)$ is the sample resistivity at 0 $T$ and $\rho(7)$ in an applied field of 70 kOe. The parent $EuBaCo_2O_{5.5}$ shows MR in the range 10–20% in the measured temperature range as expected [1], but the $NdBaCoMnO_{5.9}$ and $EuBaCoMnO_{5.7}$ compounds exhibit rather small MR value. In fact for $NdBaCoMnO_{5.9}$ the MR value is negligibly small (around −2%) even at low temperature, whereas $EuBaCoMnO_{5.7}$ exhibits a MR value close to −5% (at 80 K). The evidence of small negative MR for $EuBaCoMnO_{5.7}$ at low temperatures is considered to be related to the suppression of spin-dependent scattering of the electrons below the magnetic ordering temperature with the application of magnetic field.

## Conclusions

Oxygen-deficient 112-type ordered $NdBaCoMnO_{5.9}$ and $EuBaCoMnO_{5.7}$ perovskites were synthesized by soft-chemistry method. At room temperature there is perfect ordering between A-site cations, whereas the B-site cations are distributed randomly, in agreement with previous investigations [18–22, 33]. The valence states of Co/Mn-cations at the B-site are most probably in $Co^{2+}$, $Co^{3+}$, and $Mn^{4+}$ mixed states and majority of them interact antiferromagnetically, whereas the presence of FM interaction cannot be ruled out at low temperature. As a matter of fact the prominent FM $T_C$, insulator–metal transition and the large MR effect disappear completely for the Mn-substituted phases, in contrast to the parent cobaltites. However, the nature of magnetic interactions at low temperature varies with the nature of rare earth ions. $NdBaCoMnO_{5.9}$ is AFM below room temperature, whereas $EuBaCoMnO_{5.7}$ sample shows weak ferromagnetism as well as MR effects at low temperature due to electronic phase separation. The system appears to be phase separated into FM clusters and AFM matrix. The $M(H)$ measurements also support this assumption. In addition, the electron transport properties of both Mn-doped compounds reveal the presence of insulating phase at low temperature irrespective of their magnetic behavior.

**Acknowledgements** The authors gratefully acknowledge the CNRS and the Ministry of Education and Research for financial support. AKK thanks Prof A. Ojha, for faculty research grants.

## References

1. Martin C, Maignan A, Pelloquin P, Nguyen N, Raveau B (1997) Appl Phys Lett 71:1421
2. Maignan A, Martin C, Pelloquin D, Nguyen N, Raveau B (1999) J Solid State Chem 142:247
3. Vogt T, Woodward PM, Karen P, Hunter BA, Henning P, Moodenbaugh AR (2000) Phys Rev Lett 84:2969
4. Burley JC, Mitchell JF, Short S, Miller D, Tang Y (2003) J Solid State Chem 170:339
5. Roy S, Dubenko IS, Khan M, Condon EM, Craig J, Ali N (2005) Phys Rev B 71:024419
6. Pralong V, Caignaert V, Hebert S, Maignan A, Raveau B (2006) Solid State Ion 177:1879
7. Kundu AK, Rautama E-L, Boullay P, Caignaert V, Pralong V, Raveau B (2007) Phys Rev B 76:184432
8. Seikh MM, Simon C, Caignaert V, Pralong V, Lepetit MB, Boudin S, Raveau B (2008) Chem Mater 20:231
9. Luetkens H, Stingciu M, Pashkevich YG, Conder K, Pomjakushina E, Gusev AA, Lamonova KV, Lemmens P, Klauss HH (2008) Phys Rev Lett 101:017601
10. Kundu AK, Raveau B, Caignaert V, Rautama E-L, Pralong V (2009) J Phys Condens Matter 21:056007
11. Chernyshov D, Rozenberg G, Greenberg E, Pomyakushina E, Dmitriev V (2009) Phys Rev Lett 103:125501
12. Teraoka Y, Nobunaga T, Okamoto K, Miura N, Yamazoe N (1991) Solid State Ion 48:207

13. Kruidhof H, Bouwmeester HJM, van Doorn RHE, Burggraaf AJ (1993) Solid State Ion 63:816
14. van Doorn RHE, Burggraaf AJ (2000) Solid State Ion 128:65
15. Kim G, Wang S, Jacobson AJ, Reimus L, Brodersen P, Mims CA (2007) J Mater Chem 17:2500
16. Chavez E, Mueller M, Mogni L, Caneiro A (2009) J Phys Conf Ser 167:012043
17. Er-Rakho L, Michel C, Lacorre P, Raveau B (1988) J Solid State Chem 73:531
18. Barbey L, Nguyen N, Caignaert V, Hervieu M, Raveau B (1992) Mater Res Bull 27:295
19. Zhou W (1994) Chem Mater 6:441
20. Barbey L, Nguyen N, Caignaert V, Studer F, Raveau B (1994) J Solid State Chem 112:148
21. Raveau B, Simon C, Pralong V, Caignaert V, Lefevre F-X (2006) Solid State Commun 139:301
22. Raveau B, Simon C, Caignaert V, Pralong V, Lefevre F-X (2006) J Phys Condens Matter 18:10237
23. Kim J-H, Manthiram A (2009) Electrochim Acta 54:7551
24. Jacob M, Hansen S, Sturefelt S (1990) Microsc Microanal Microstruct 1:319
25. Shivkumar C, Hegde MS, Subbanna GN (1996) Bull Mater Sci 19:607
26. Huang Q, Karen P, Karen VL, Kjekshus A, Lynn JW, Mighell AD, Sora IN, Rosov N, Santoro A (1994) J Solid State Chem 108:80
27. Ruiz-Gonzalez L, Boulahya K, Parras M, Alonso J, González-Calbet JM (2002) Chem Eur J 8:5694
28. Suescun L, Jones CY, Cardoso CA, Lynn JW, Toby BH, Aranjo-M FM, Lima OF, Pardo H, Mombru AW (2005) Phys Rev B 71:144405
29. Klyndyuk AI (2009) Phys Solid State 51:270
30. Klyndyuk AI (2009) Phys Solid State 51:657
31. Klyndyuk AI (2009) Inorg Mater 45:942
32. Karen P, Suard E, Fauth F, Woodward PM (2004) Solid State Sci 6:1195
33. Snedden A, Wright AJ, Greaves C (2008) Mater Res Bull 43:2403
34. Rietveld HM (1969) J Appl Crystallogr 2:65
35. Trukhanov SV, Troyanchuk IO, Hervieu M, Szymczak H, Barner K (2002) Phys Rev B 66:184424
36. Goodenough JB (1976) Magnetism and the chemical bond. R. E. Krieger Publishing Company, Huntington
37. Troyanchuk IO, Lobanovsky LS, Khalyavin DD, Pastushonok SN, Szymczak H (2000) J Mag Mag Mater 210:63
38. Chang CL, Tai MF, Chung TW, Lee FY, Su YW, Liu SY, Hwang CS, Tseng PK, Shi JB (2000) J Mag Mag Mater 209:240
39. Park J-H, Cheong S-W, Chen CT (1997) Phys Rev B 55:11072
40. Kundu AK, Nordblad P, Rao CNR (2005) Phys Rev B 72:144423
41. Kundu AK, Nordblad P, Rao CNR (2006) J Phys Condens Matter 18:4809